Naval Research Laboratory

Washington, DC 20375-5320

NRL/MR/6750--09-9192

Fokker-Planck Model for Thermal Smoothing in Inhomogeneous Laser-Matter Interactions

MICHAEL J. KESKINEN

Charged Particle Physics Branch
Plasma Physics Division

July 24, 2009

Approved for public release; distribution is unlimited.

REPORT DOCUMENTATION PAGE

Form Approved
OMB No. 0704-0188

Public reporting burden for this collection of information is estimated to average 1 hour per response, including the time for reviewing instructions, searching existing data sources, gathering and maintaining the data needed, and completing and reviewing this collection of information. Send comments regarding this burden estimate or any other aspect of this collection of information, including suggestions for reducing this burden to Department of Defense, Washington Headquarters Services, Directorate for Information Operations and Reports (0704-0188), 1215 Jefferson Davis Highway, Suite 1204, Arlington, VA 22202-4302. Respondents should be aware that notwithstanding any other provision of law, no person shall be subject to any penalty for failing to comply with a collection of information if it does not display a currently valid OMB control number. **PLEASE DO NOT RETURN YOUR FORM TO THE ABOVE ADDRESS.**

1. REPORT DATE *(DD-MM-YYYY)*	**2. REPORT TYPE**	**3. DATES COVERED** *(From - To)*
24-07-2009	Memorandum Report	

4. TITLE AND SUBTITLE

Fokker-Planck Model for Thermal Smoothing in Inhomogeneous Laser-Matter Interactions

5a. CONTRACT NUMBER

5b. GRANT NUMBER

5c. PROGRAM ELEMENT NUMBER

6. AUTHOR(S)

Michael J. Keskinen

5d. PROJECT NUMBER
67-9387-F7

5e. TASK NUMBER

5f. WORK UNIT NUMBER

7. PERFORMING ORGANIZATION NAME(S) AND ADDRESS(ES)

Naval Research Laboratory
4555 Overlook Avenue, SW
Washington, DC 20375-5320

8. PERFORMING ORGANIZATION REPORT NUMBER

NRL/MR/6750--09-9192

9. SPONSORING / MONITORING AGENCY NAME(S) AND ADDRESS(ES)

Department of Energy
1000 Independence Avenue, SW
Washington, DC 20585

10. SPONSOR / MONITOR'S ACRONYM(S)

11. SPONSOR / MONITOR'S REPORT NUMBER(S)

12. DISTRIBUTION / AVAILABILITY STATEMENT

Approved for public release; distribution is unlimited.

13. SUPPLEMENTARY NOTES

14. ABSTRACT

Using a fully kinetic 2D Fokker-Planck model, the generation and evolution of ion density perturbations from nonuniform laser deposition in a plasma slab have been studied. It is found that significant smoothing of the ion density perturbations from nonuniform optically smoothed single beam laser deposition can be achieved on hydrodynamic time scales over a long range of scale sizes. In addition, it is observed that the Fokker-Planck model predicts more smoothing than the hydrodynamic Spitzer model.

15. SUBJECT TERMS

Laser
Inertial fusion
Heat transfer

16. SECURITY CLASSIFICATION OF:			**17. LIMITATION OF ABSTRACT**	**18. NUMBER OF PAGES**	**19a. NAME OF RESPONSIBLE PERSON**
a. REPORT	**b. ABSTRACT**	**c. THIS PAGE**			Michael J. Keskinen
Unclassified	Unclassified	Unclassified	UL	16	**19b. TELEPHONE NUMBER** *(include area code)* (202) 767-3215

Standard Form 298 (Rev. 8-98)
Prescribed by ANSI Std. Z39.18

Fokker-Planck Model for Thermal Smoothing in Inhomogeneous Laser-Matter Interactions

Energy transport in laser-produced plasmas is an important issue in current high energy density plasma research, e.g., inertial confinement fusion (ICF) [1,2], femtosecond laser interactions with solids, and laboratory simulations of astrophysical phenomena using lasers.

In ICF, laser energy, absorbed in the hot, low density corona, must be effectively conducted toward colder, higher density regions of the target. A large inward heat flux from the critical surface, toward higher density regions, implies that newly heated material at the surface of the cold target will expand outward rapidly leading to large fuel compression. Large compressions can lead to higher fusion gains. A limitation in ICF is pellet degradation and disruption due to the Rayleigh-Taylor (RT) instability where a hot, low-density plasma is used to compress and accelerate a cold, high density plasma. The RT instability can be seeded by laser nonuniformities from single or multiple beams and target surface irregularities [1,2]. Single beam nonuniformities are the most detrimental to RT seeding and contribute to imprint through perturbations in the laser driven shock front and acceleration in the post shock region. Short wavelength laser nonuniformities δI/I may be reduced [1,2] due to thermal diffusion and smoothing such that δP/P $\leq$ δI/I where δP/P is the pressure nonuniformity at the ablation surface which can seed the RT instability. However longer wavelength laser nonuniformities may not be reduced by thermal diffusion alone [3,4]. In order to reduce the amplitudes of the laser uniformities,

Manuscript approved June 4, 2009.

techniques for laser optical smoothing have been developed, e.g., induced spatial incoherence [5], spectral dispersion [6], and distributed phase plates [7].

Models for nonuniform laser-driven spatial and temporal heat flow evolution, over a large range of scale sizes, are important for ICF. It is well known that that the measured heat flux is [8] below the flux predicted by classical electron thermal conduction. Strong inhibition of thermal transport below classical thermal conduction seems to exist in both long and short pulse laser deposition and in both high and low Z plasmas. In addition, the measured heat transport seems to be reduced both inward toward higher density regions and laterally toward the exterior. Several models have been advanced to explain the reduced heat flux in ICF experiments, e.g., ion acoustic turbulence [9], DC magnetic field effects [10], and kinetic theory in steep temperature gradients [11-15]. It has been shown [16,17] that hydrodynamic fluid models are not accurate to describe heat flow when $k\lambda_{mfp} \geq 1/80$ where $2\pi k^{-1}$ is the scale size of the temperature or pressure and λ_{mfp} is the collisional mean free path. When this inequality is fulfilled, a kinetic model, e.g., a Vlasov Fokker-Planck (FP) formulation, must be used.

Some initial work has been performed using both hydrodynamic fluid models [3, 19-21] and FP models [16,18], to study thermal smoothing and heat flow generated by nonuniform, inhomogeneous laser deposition for ICF applications. Previous FP studies [16,18] have been primarily devoted to the problem of the smoothing of

electron temperature perturbations with a single scale size resulting from nonuniform laser deposition. The smoothing of ion density perturbations, resulting from nonuniform laser depostion, have not been studied quantitatively using FP models over a range of scale sizes. These ion density perturbations, at the ablation surface, can seed longer time scale Rayleigh-Taylor instabilities. However, laser deposition, resulting from optically-smoothed lasers, can be structured over a broad range of spatial and temporal scales [5-7]. An outstanding problem is a kinetic model for the generation and evolution of ion density perturbations when $\mathrm{k}\lambda_{\mathrm{mfp}} \geq 1/80$.

The objective of this paper is to study ion density perturbations, using a fully kinetic FP model, resulting from simulated nonuniform optically-smoothed laser deposition for a wide range of scale sizes. It is found that significant smoothing of ion density perturbations can be achieved on hydrodynamic time scales for a range of spatial scale sizes.

It is assumed that, to lowest order, the electron and ion distribution functions f are weakly anisotropic. As a result, we make the standard decomposition [22] with $\mathrm{f}_\alpha = \mathrm{f}_{0\alpha} + (\mathrm{v}/\mathrm{v}) \cdot \mathbf{f}_{1\alpha}$ with $\alpha = \mathrm{e}, \mathrm{i}$. For the electrons, in the frame of the ions:

$$\frac{d\mathrm{f}_{0e}}{dt} + \frac{v}{3}\nabla\cdot\mathbf{f}_{1e} - \nabla\cdot\mathbf{v}_i \frac{v}{3}\frac{\partial f_{0e}}{\partial v} + \frac{1}{3v^2}\frac{e}{m_e}\frac{\partial}{\partial v}\left(v^2\left(\mathbf{E}+\mathbf{E}_p\right)\cdot\mathbf{f}_{1e}\right) = \frac{Y_{ee}}{v^2}\frac{\partial}{\partial v}\left(A_{1e}f_{0e} + A_{2e}\frac{\partial f_{0e}}{\partial v}\right) + \mathrm{S} \tag{1}$$

$$\frac{\partial \mathbf{f}_{1e}}{\partial t} + v\nabla f_{0e} + \frac{e}{m_e}\left(\mathbf{E}+\mathbf{E}_p\right)\frac{\partial f_{0e}}{\partial v} = -\nu_{ei}^{*}\mathbf{f}_{1e} \tag{2}$$

where $\mathrm{Y_{ee}} = 4\pi(\mathrm{e}^2/4\pi\mathrm{m_e})^2\ln\Lambda_{\mathrm{ee}}$, the laser heating source term S can be written as

$S = (Y_{ee}/v^2)\partial/\partial v[(n_i/6v)(Z^2 ln\Lambda_{ei}/ln\Lambda_{ee})(1/\omega^2 + \nu_{ei}^2)(eE_0^2/m_e)^2]\partial f_{0e}/\partial v$ and $d/dt = \partial/\partial t + \mathbf{v}_i \cdot \nabla$. In addition, $\nu_{ei}^* = (4\pi\phi n e^4 Z^*/m^2 v^3) ln\Lambda$, $\nu_{ee} = (4\pi n e^4/m^2 v^3) ln\Lambda$, $\phi = (Z^* + 4.2/(Z^* + 0.24)$, and $Z^* = \langle Z^2 \rangle / \langle Z \rangle$. Here the angle brackets denote an average over all ion species. In Eq. (1), $\mathbf{v}_i$ is the average ion velocity derived from Eq. (4)-(5). The quantities A_{1e} and A_{2e} have been previously defined [16, 22]. The ponderomotive electric field $\mathbf{E}_p = (e/4m_e\omega^2)\nabla|\mathbf{E}_0|^2$. In Eq. (1)-(2), $\mathbf{E}$ is taken to be electrostatic and $\mathbf{E}_0$ is the laser electromagnetic electric field. Here S represents laser inverse bremstrahllung absorption using the Langdon prescription [23].

The laser electromagnetic field is computed using a wave equation for the slow evolution of the wave field. The equation for the slow E_0 can be written:

$$\left[\frac{\partial}{\partial t} - \frac{ic^2}{2\omega_0}\left(\frac{\partial^2}{\partial x^2} + \frac{\partial^2}{\partial z^2}\right) - i\omega_0\left(\epsilon_r - i\epsilon_i\right)\right] E_0 = 0 \tag{3}$$

where $\epsilon_r = 1 - n_e(z)/n_c$ and $\epsilon_i = (\nu_{ei}/\omega_0)n_e(z)/n_c$. In the transverse x-direction the wavenumbers k_x for the spectral content of the laser electromagnetic field are constructed to simulate a set of beamlets generated by optical smoothing. The beamlets are then overlapped at the target plane using a lens of focal length f. The diffraction profile at the target plane will have a width $d = 2\lambda f/D_1$ where λ is the laser wavelength and D_1 is the beamlet width in which the laser intensity is assumed uniform. The transverse wavenumbers are then given by $k_{xn} = nD_1/\lambda f$ with n=1,2,..... In this preliminary study, f=40 m, $\lambda = 0.25\mu$m, $D_1 = 75$ mm so that $d = 200\mu$m. The set of transverse wavelengths used are $\lambda_n = 100\mu m/n$ with

n=1,.....40. The complex amplitude of each beamlet is taken to obey Gaussian probability statistics with independent random fluctuations with a coherence time τ_c of 2 ps. A range of laser rise times of 10 - 100 ps were used.

For the ion species we have:

$$\frac{\partial \mathrm{f}_{0i}}{\partial t} + \frac{v}{3}\nabla \cdot \mathbf{f}_{1i} - + \frac{1}{3v^2}\frac{Ze}{m_i}\frac{\partial}{\partial v}\left(v^2 \mathbf{E} \cdot \mathbf{f}_{1i}\right) = \frac{Y_{ii}}{v^2}\frac{\partial}{\partial v}\left(A_{1i} f_{0i} + A_{2i}\frac{\partial f_{0i}}{\partial v}\right) + S_{ie} \quad (4)$$

$$\frac{\partial \mathbf{f}_{1i}}{\partial t} + v\nabla f_{0i} + \frac{eZ\mathbf{E}}{m_i}\frac{\partial f_{0i}}{\partial v} = -\nu_{ie}\mathbf{f}_{1i} \quad (5)$$

where $\mathrm{S}_{ie} = -(\mathrm{m}_e/\mathrm{m}_i)(\nu_{ei}/\mathrm{v}^2)\partial/\partial \mathrm{v}((\mathrm{v}^2\mathrm{T}_e/\mathrm{m}_i)\partial \mathrm{f}_{0i}/\partial \mathrm{v} + \mathrm{v}^3\mathrm{f}_{0i})$

The electric field $\mathbf{E}$ in Eq. (1),(2),(4),(5) is found from the zero current condition, i.e., $\mathbf{J} = 0$. We have numerically solved the model equation set consisting of Eq. (1)-(5). The 2D fully kinetic Fokker-Planck code is solved using an alternating-direction implicit method. The peak vacuum laser intensity is $4 \times 10^{14}\mathrm{W/cm}^2$ and is assumed to be normally incident in the x-direction. The plasma parameters used are such that the ion acoustic transit time $\mathrm{t_s} \simeq 50 - 125\mathrm{ps}$ and the thermal diffusion time $\mathrm{t_{th}} \simeq 20 - 100\mathrm{ps}$.

Fig. 1 shows the initial electron temperature and density profiles used in the simulation. The critical surface is located initially at approximately at $\mathrm{z} = 100\mu\mathrm{m}$. The ablation surface is located initially at approximately at $\mathrm{z} = 180\mu\mathrm{m}$. The initial electron temperature $\mathrm{T_e}$ is taken to be 230 eV with the initial ion temperature $\mathrm{T_i} = 0$. The initial temperature and density is assumed to be uniform in the

transverse x-direction.

Fig. 2 shows the longitudinal and transverse intensity profiles used to simulate optically-smoothed laser deposition. The longitudinal structure is consistent with an Airy pattern while the transverse structure is random both in space and time and is due to simulated optical smoothing. These intensity profiles are used in the source term in Eq. (1). A single Gaussian beam with a full width at half maximum of 80 μm is used.

Fig. 3 shows the 2D variation of the FP electron temperature T_e at t=420 ps with a laser coherence time of 2 ps. The evolution of the electron temperarure also shows both longitudinal and transverse structure. It is found that ponderomotive effects are important only in the underdense plasma, i.e., for $z \leq 100\mu$m. Significant smoothing of the electron temperature perturbations is seen from the critical to ablation surface.

Fig. 4 shows the 2D variation of the ion density n_i at t=420 ps. It is found that structure at and near the critical surface develops in the ion density. This structure is caused by a hydrodynamic instability [24] due to a combination of a pressure gradient and a density gradient and is related to a buoyancy-driven Rayleigh-Taylor like process. If the ion density perturbation is written as $\delta n_i/n_0 \propto \exp(ik_x x + \gamma t)$ then a hydrodynamic instabilty will grow with growth rate $\gamma = [(C_s^2/\gamma_p)(4k_x^2L^2/1 + 4k_x^2L^2)(1/\gamma_p L_p^2 - 1/L_p L)]^{1/2}$. Here $1/L_p = \partial \ln p/\partial z$, $1/L =$

$\partial \mathrm{lnn}_i/\partial \mathrm{z}$, C_s is the ion sound speed, and γ_p is the polytropic index. It is found that this structure is persistent and is generated for a range of laser rise times and coherence times. This hydrodynamic instability is modulated in the transverse direction by the optically smoothed nature of the laser deposition. This structure may have important consequences for thermal self-focussing processes. Significant smoothing is observed also for the ion density perturbations.

In addition, the root-mean-square σ_{rms} of the ion density perturbations was computed as a function of the longitudinal direction. The root-mean-square σ_{rms} is given by:

$$\sigma_{rms}\left(z\right) = \frac{1}{\langle n_i \rangle}\left[\frac{1}{L_X}\int dx\left(n_i - \langle n_i \rangle\right)^2\right]^{\frac{1}{2}} \tag{6}$$

where $\mathrm{L_X}$ is the system size in the transverse x-direction and the angle brackets denote spatial average. The ion density perturbations maximize near the critical surface and decrease in magnitude into the overdense region. The ion density perturbations at the ablation surface $\sigma_{rms}(\mathrm{z} = \mathrm{z}_{abl}) \leq 0.01$. The ion density perturbations at the ablation surface $\sigma_{rms}(\mathrm{z} = \mathrm{z}_{abl}) \propto \tau_c^n$ with $\mathrm{n} \simeq 0.6 - 1$ for $\tau_c \simeq 2 - 8$ps. The ion density perturbations were also computed using a Spitzer fluid code for two flux limiters, i.e., f = 0.07, 0.1. It was found that the FP model predicts more smoothing than a hydrodynamic model for both flux limiters, i.e., $\sigma_{rms}^{FP} < \sigma_{rms}^{SH}$.

In summary, using a fully kinetic 2D Fokker-Planck model, the generation and evolution of ion density perturbations from nonuniform laser deposition in a plasma

slab has been studied. It is found that significant smoothing of the ion density perturbations from nonuniform optically-smoothed single beam laser deposition can be achieved on hydrodynamic times scales over a range of scale sizes. In addition, it is observed that the Fokker-Planck model predicts more smoothing than the hydrodynamic Spitzer model. It is found that ion density structure can be caused by a hydrodynamic instabilty which is related to a buoyancy-driven Rayleigh-Taylor-like process.

We wish to thank S. Obenschain, D. Colombant, W. Manheimer, and J. Bates for useful discussions. This work was supported by the U.S. Department of Energy.

[1] J.D. Lindl, Inertial Confinement Fusion (Springer-Verlag, New York, 1998).

[2] S.E. Bodner, J. Fusion Energy, 1, 221 (1981).

[3] M.H. Emery, J.H. Orens, J.H. Gardner, and J.P. Boris, Phys. Rev. Lett., **48**, 253 (1982).

[4] J.H. Gardner and S.E. Bodner, Phys. Rev. Lett., **47**, 1137 (1981).

[5] R.H. Lehmberg and S.P. Obenschain, Opt. Commun. **46**, 27 (1983).

[6] S. Skupsky, R.W. Short, T. Kessler, R.S. Craxton, S. Letzring, and J.M. Soures, J. Appl. Phys., **66**, 3456 (1989).

[7] Y. Lin, T.J. Kessler, and G.N. Lawrence, Opt. Lett., **20**, 764 (1995).

[8] W.L. Kruer, Comments on Plasma Phys. and Controlled Fusion **5**, 69 (1979); G. Schurtz *et al.*, Phys. Rev. Lett., **98**, 095002 (2007).

[9] W. Manheimer, Phys. Fluids, **20**, 265 (1977).

[10] M. Straus, G. Hazak, D. Shvarts, and R. Craxton, Phys. Rev. A, **30**, 2627 (1984); A.V. Brantov *et al.*, Phys. Plasmas **10**, 4633 (2003); Ph. Nicolai *et al.*, Phys. Plasmas **13**, 032701 (2006).

[11] J. Matte and J. Virmont, Phys. Rev. Lett., **49**, 1936 (1982).

[12] J. Matte, T.W. Johnston, J. Delettrez, and R.L. McCrory, Phys. Rev. Lett., **53**, 1461 (1984).

[13] J. Luciani, P. Mora, and J. Virmont, Phys. Rev. Lett., **51**, 1664 (1983).

[14] J. Albritton, Phys. Rev. Lett. **50**, 2078 (1983).

[15] G.J. Rickard, A.R. Bell, and E.M. Epperlein, Phys. Rev. Lett., **62**, 2687 (1989).

[16] E. Epperlein, G. Rickard, and A. Bell, Phys. Rev. Lett., **61**, 2453 (1988).

[17] A. Sunahara, J. Delettrez, J. Stoeckl, R. Short, and S. Skupsky Phys. Rev. Lett., **91**, 095003-1 (2003).

[18] I.R. Williams, G.J. Rickard, and A.R. Bell, Laser Part. Beams, **9**, 247 (1991).

[19] V.K. Senecha, A.V. Brantov, V. Yu. Bychenkov, and V.T. Tikhonchuk, Phys. Rev. E **57**, 978 (1998).

[20] O. V. Batishchev, V. Yu. Bychenkov, F. Detering, W. Rozmus, R. Sydora, C.E. Capjack, and V.N. Novikov, Phys. Plasmas **9**, 2302 (2002).

[21] J.-L. Feugeas, Ph. Nicolaï, X. Ribeyre, G. Schurtz, V. Tikhonchuk, and M. Grech, Phys. Plasmas **15**, 062701 (2008).

[22] I. Shkarofsky, T. Johnston, and M. Bachynski, *The Particle Kinetics of Plasmas*, Reading: Addison-Wesley.

[23] A. Langdon, Phys. Rev. Lett. **44**, 575 (1980).

[24] R.P. Drake, Plasma Phys. Control. Fusion **47**, B419 (2005).

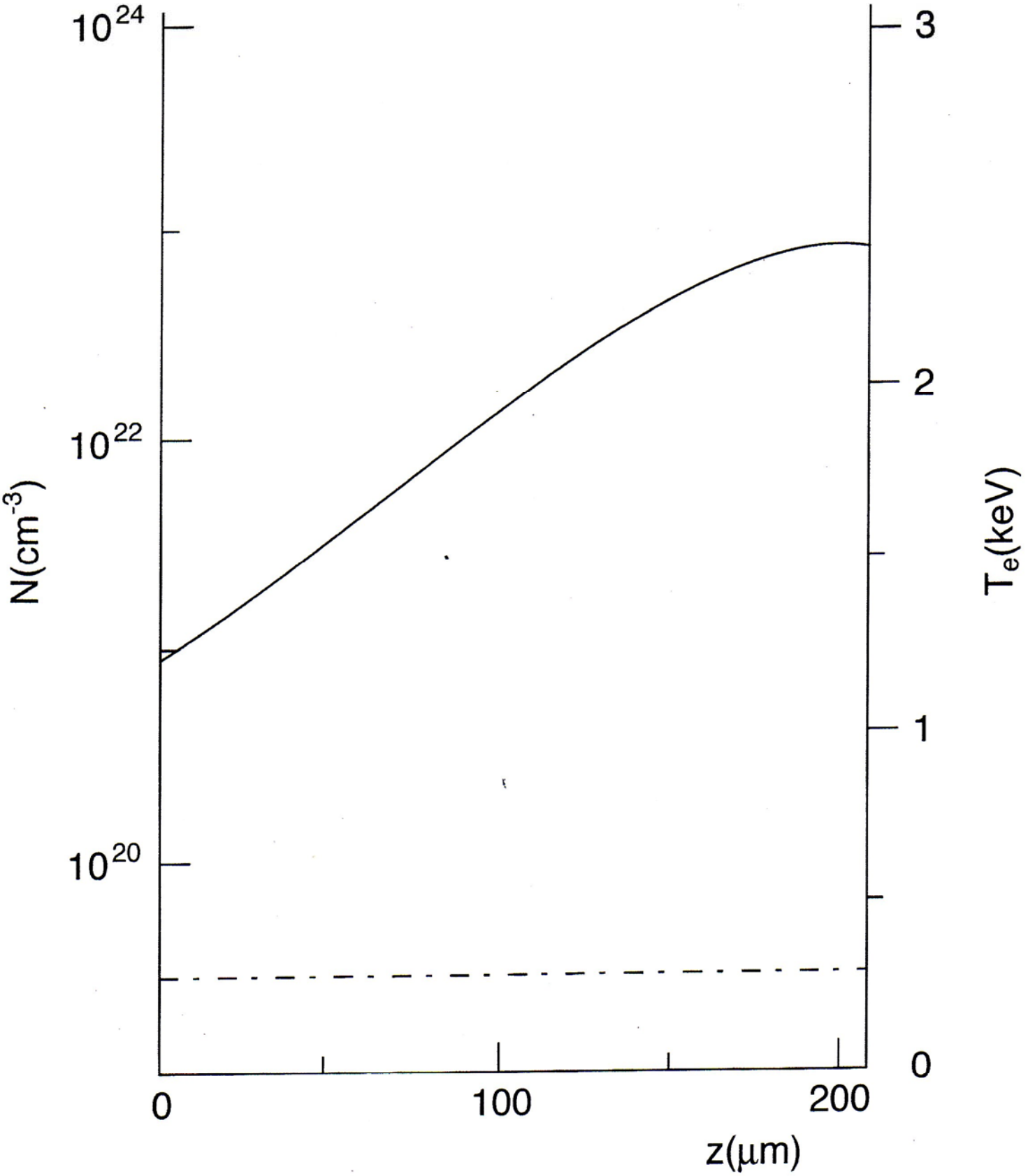

Figure 1

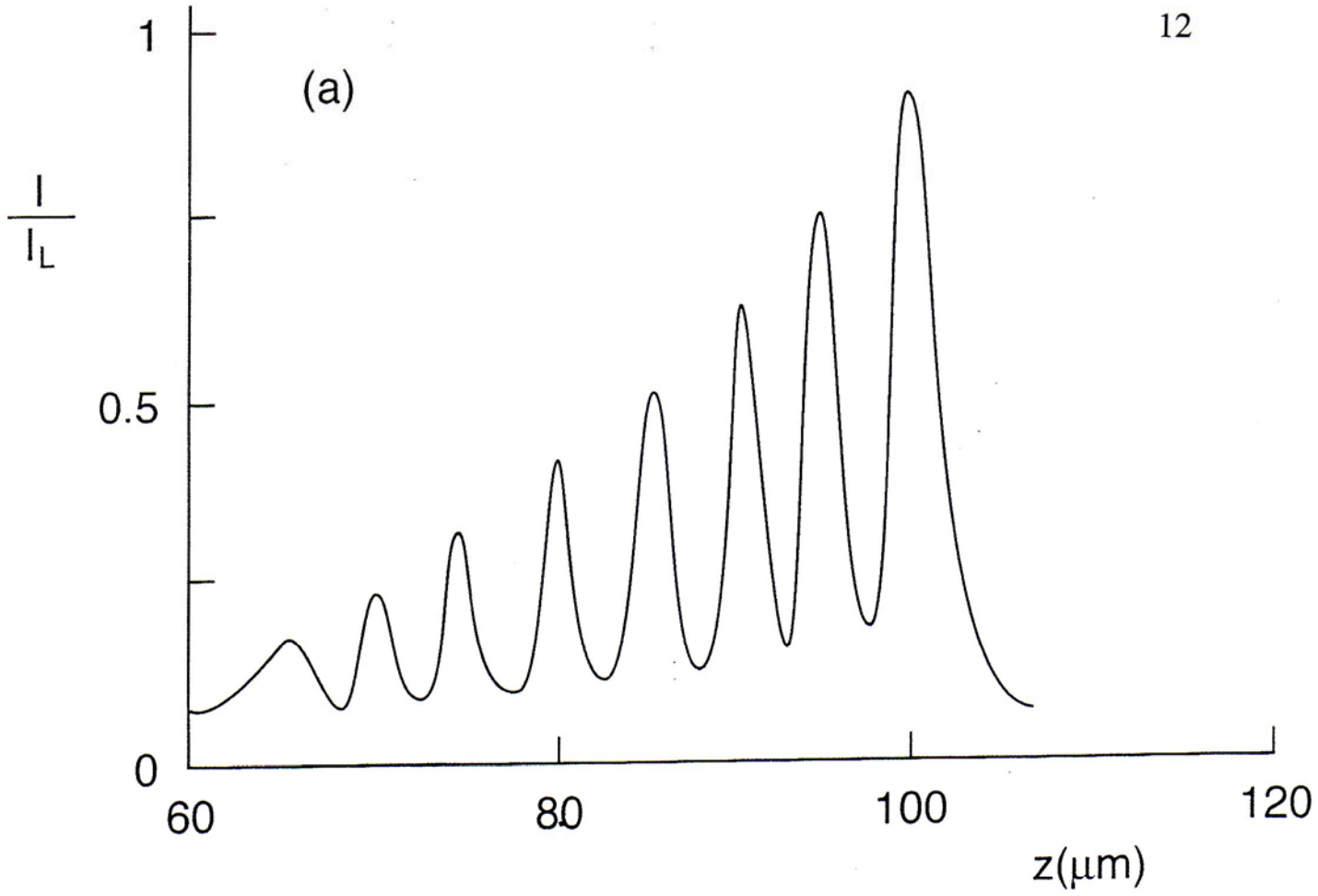

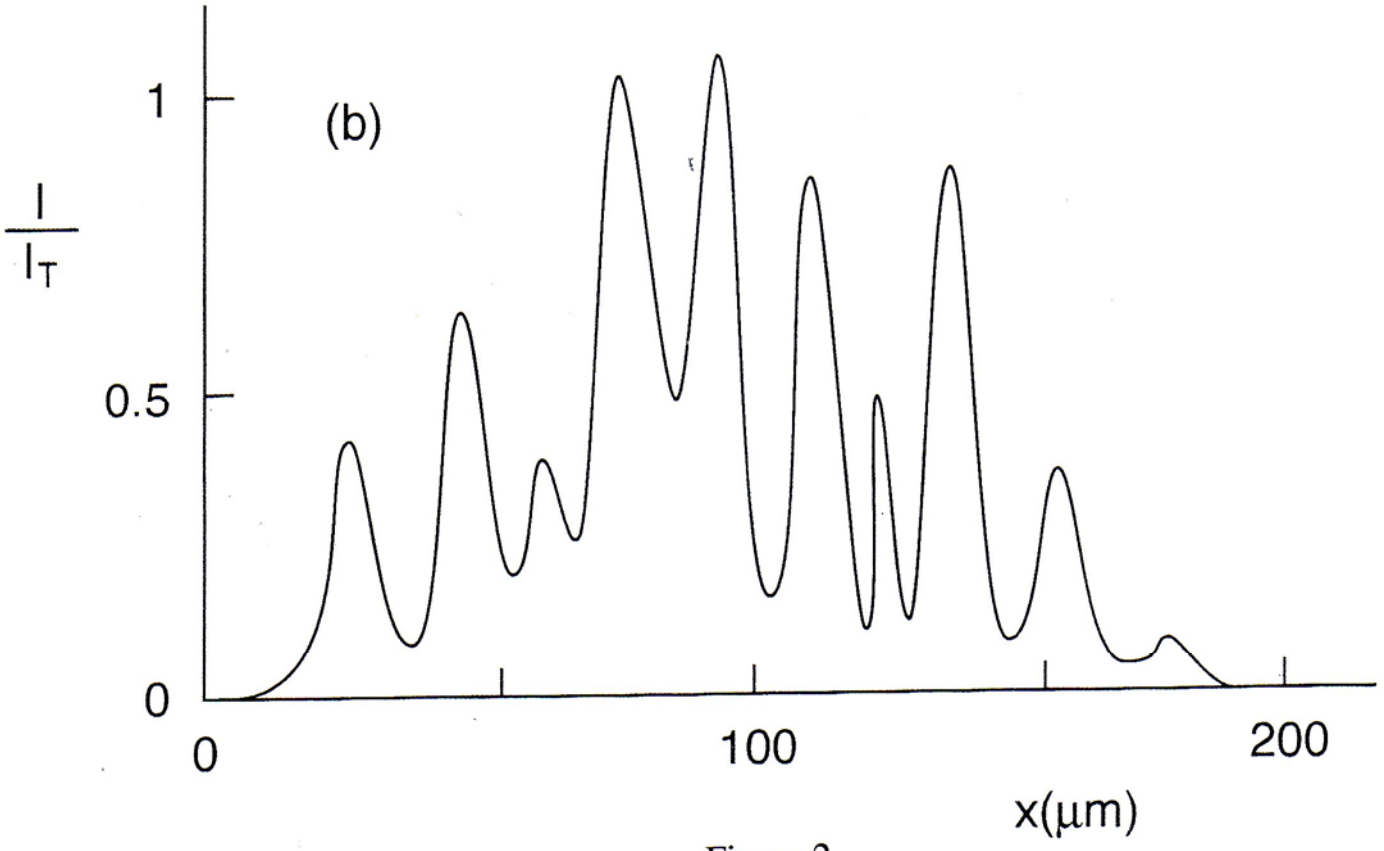

Figure 2

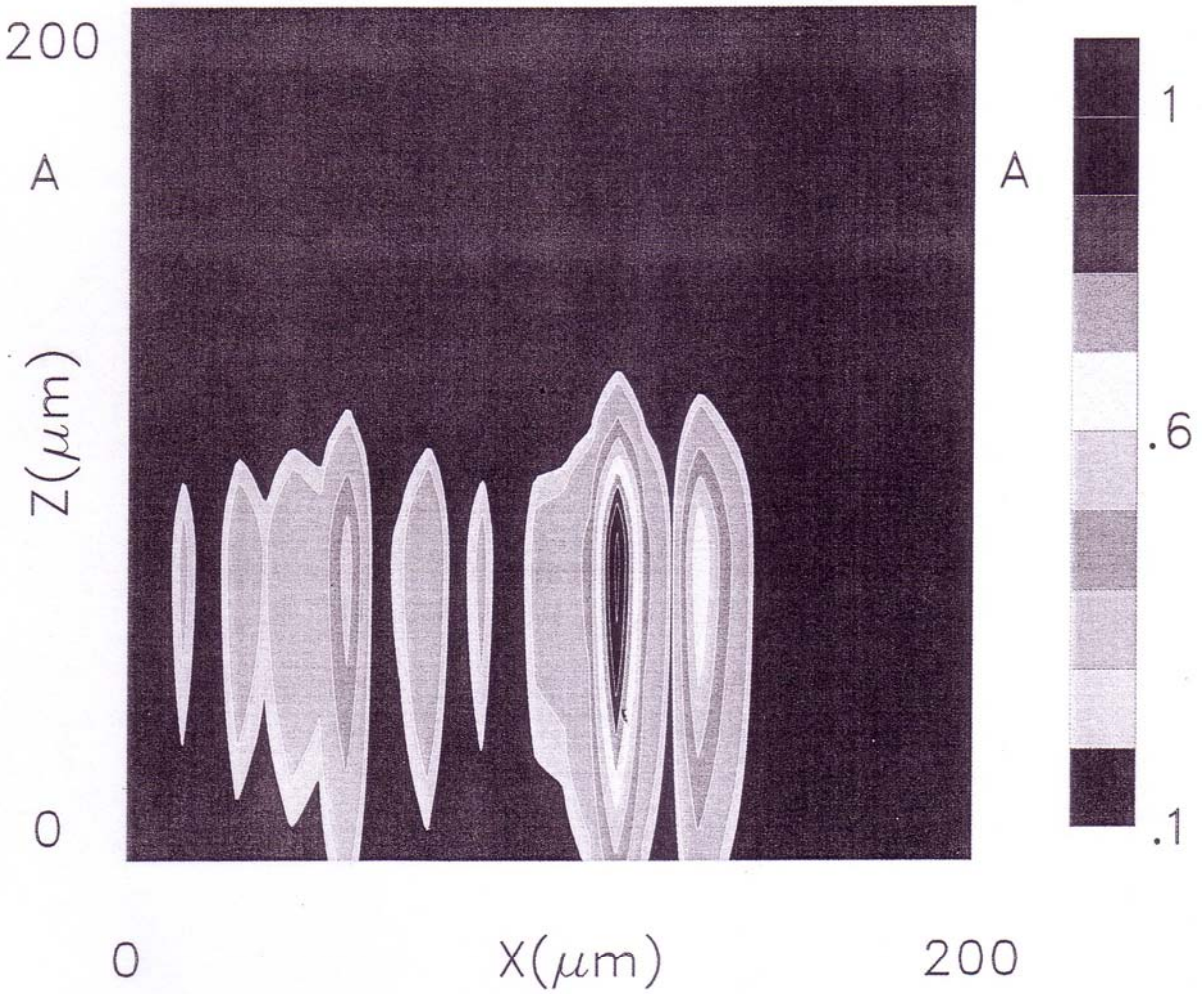

Figure 3

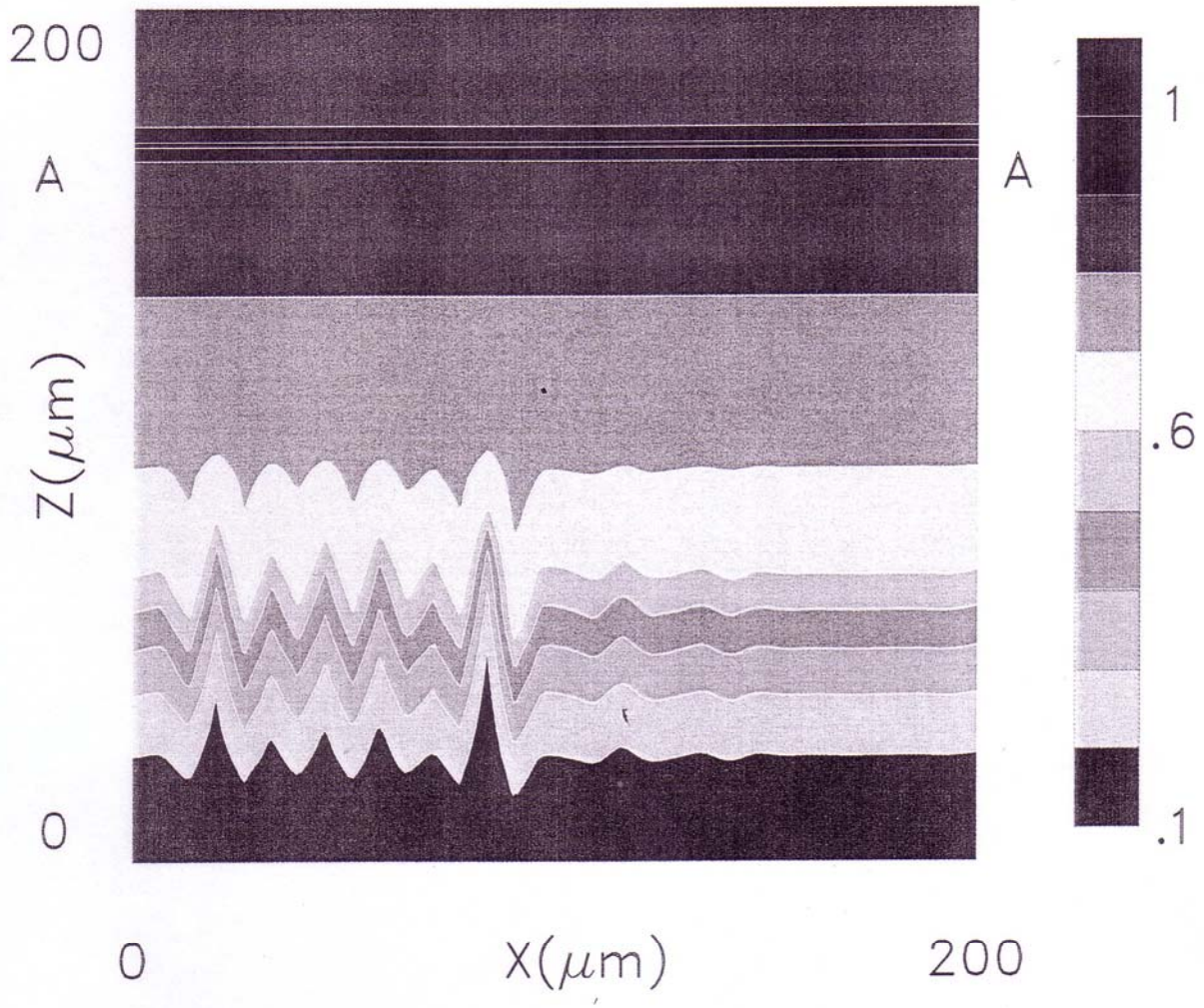

Figure 4